THE DYNAMIC DIGITAL PHOTOGRAMMETRIC MEASUREMENT AND VISUALISATION OF A 21M WIND TURBINE ROTOR BLADE UNDERGOING STRUCTURAL ANALYSIS.

S. Robson and H. B. Setan.

Engineering Surveying Research Centre
Department of Civil Engineering
City University London, EC1V OHB
UNITED KINGDOM
Tel: +44 171 477 8000 xtn 3682
Facsimile: +44 171 8570
Email: S.Robson@city.ac.uk

Faculty of Surveying and Real Estate
Universiti Teknologi Malaysia
Locked Bag 791, 80990 Johor Bahru
MALAYSIA
Tel: +60 7-557 6160 xtn 2813
Facsimile: +60 7 55 66 163

ISPRS Commission V, Working Group 3

KEY WORDS: Engineering, Metrology, Monitoring, Deformation Analysis, Digital Photogrammetry.

ABSTRACT

The testing and monitoring of structural components is standard practice in the construction industry, its aims being the establishment of specifications, conformance to design and subsequent monitoring during and after construction. Conventional structural monitoring methods include the use of a variety of instrumentation, for example, strain gauges, electro-levels and deflection gauges. These are only capable of measuring deformation in, at most, two dimensions. Digital photogrammetry combined with conventional survey can provide a complimentary non-contact measurement technique able to quickly provide three dimensional spatial information of verifiable quality.

1. INTRODUCTION

Recent advances in camera sensor technology and computer hardware mean that non-contact, on-line inspection methods based on automated digital image measurement offer much potential. Through international research and development digital imaging technologies allied with photogrammetric techniques are becoming capable of achieving object space precision of the order of 1:200,000 and better (Beyer 1995). Collaborative research at City University has produced a suite of semi-automated calibration, image capture and measurement techniques which allow the accurate and reliable computation of 3D co-ordinates within small object volumes (Robson et al 1995).

The work described in this paper is based on the photogrammetric co-ordination of retro-reflective targets using a research orientated spatial acquisition system which can employ between three and six multiplexed analog CCD cameras. Target images are rapidly measured and correlated to sub-pixel accuracies (Clarke et al 1995) from which 3D co-ordinates may be automatically computed using photogrammetric bundle adjustment techniques. The algorithms for calibration of the cameras used in this process have been modified to include the variation of lens distortion with object space distance where appropriate data are available (Fraser and Shortis 1992). Physical and statistical checking procedures are used throughout to ensure that the resultant data are accurate, precise and reliable (Cooper and Robson 1994).

The potential of these low cost videometric components is now being explored within the structural monitoring programme at City University. Some initial trial experiments have been conducted to asses the ability of the system to measure simple structures such as an I-Beam under static loading (Robson and Cooper 1995), and fine art wood panel paintings under changes in environmental condition (Robson et al 1995). This paper describes the system's application to the more complicated case of the loading of a large composite wind turbine rotor blade.

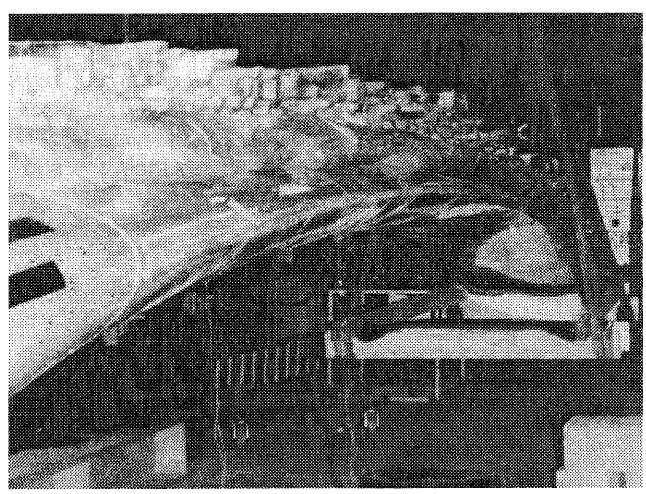

Figure 1 A wind turbine blade under test.

2. STRUCTURAL TESTING

City University is a key centre for the testing of large composite wind turbine rotor blades. Full scale structural testing of rotor blades may be required for design verification or for assessing the structural integrity of the rotor blade. Various types of testing process are used including fatigue tests, static tests and modal tests. The example application described in this paper is a distributed static loading test of a 21m long wind turbine rotor blade. The primary aim of the experiment is to make a verification of design stress distribution.

Table 1 Rotor blade load increments.

7th June 1995		10th June 1995	
Epoch	% design load	Epoch	% design load
0	0	10	100
1	50	11	150
2	100	12	175J
3	150	13	200
-	-	14	200J
-	-	15	225J
-	-	16	250J
-	-	17	250J

A structural test of this type involves loading the blade according to a design distribution which reflects wind load. Whilst several suitable test methods exist, in this case, the blade was firmly fixed at its root to a jig, sand bags and lead ingots were then incrementally placed on the blade surface in a configuration designed to reflect wind loading. Table 1 details the loading increments applied to the rotor blade. The suffix 'J' on the later epochs indicates that the angle of the supporting jig was altered by means of hydraulic jacks to allow the static load to be applied without the tip of the rotor blade touching the laboratory floor. The final epoch (17) consisted of a series of small changes in the hydraulic jacks as the rotor blade was allowed to fail due to creep.

At each increment in design load, measurements of strain and deflection were made at strategic locations on and within the rotor blade. Deflection measurements were made by conventional intersection survey. Two Zeiss Elta 2 total stations were used to coordinate several pre-targeted points located at specific points along the blade length. Table 2 shows the RMS location of these targets in all three coordinate axes. These values meet the sub-

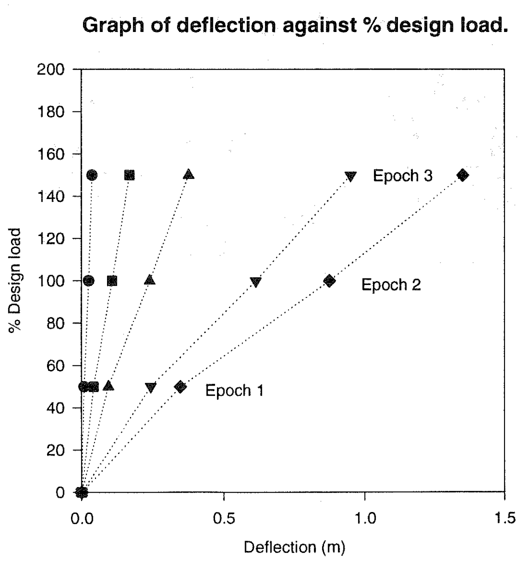

Figure 2 Measurements of deflection against design load for the targeted points along the blade length.

millimetre specification since only deflection measurements, corresponding to the Z axis, were required. These measurements are conventionally plotted against % design load to give the graph in figure 2.

Table 2 Target location precision by survey intersection

Axis	X	Y	Z
Coordinate RMS (mm)	1.71	2.01	0.70

3. PHOTOGRAMMETRIC DATA ACQUISITION

The research orientated digital photogrammetric system available at the time of testing was not capable of measuring the complete length of the blade to sub-millimetre precision. Instead a small 3m long region of interest at the major change in section near the root of the rotor blade was selected. This area was spray painted with matt-black cellulose paint to reduce surface glare before targeting with 62 3mm diameter retro-reflective targets. Ten larger retro-targets were mounted independently of the test structure and coordinated by intersection with the Zeiss Elta 2 instruments to provide a stable control network. Three additional targets were located on the supporting jig to provide a measure of the stability of the rotor blade mounting.

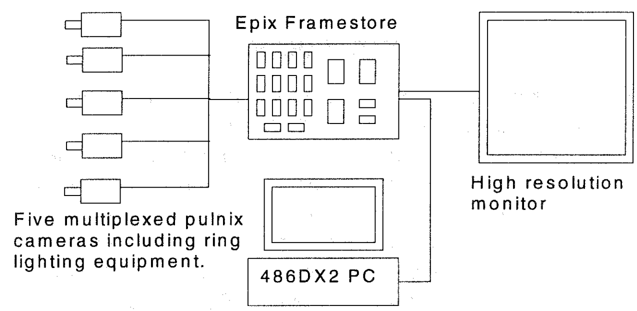

Figure 3 Schematic diagram of the imaging system

Five Pulnix TM6CN interline CCD cameras were used to image the targeted volume. Figure 4 illustrates the network used and the relative positions of the structural components. All five cameras were previously calibrated using optical bench techniques and straight line arrays at three different distances coinciding with the near, far and intermediate object distances. These data were then used

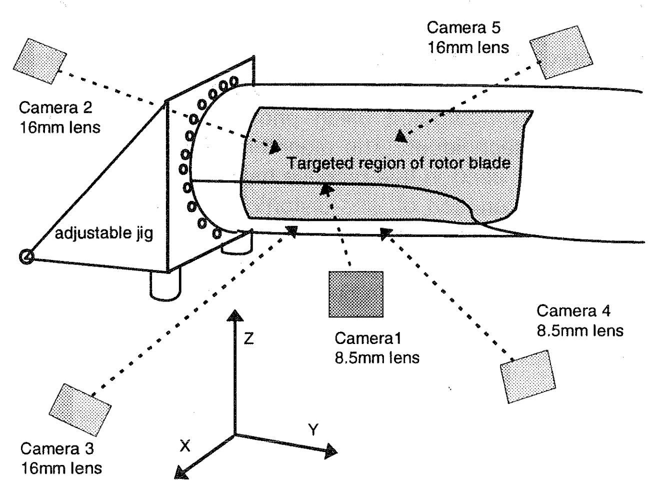

Figure 4 The photogrammetric network used to measure a portion of the turbine blade.

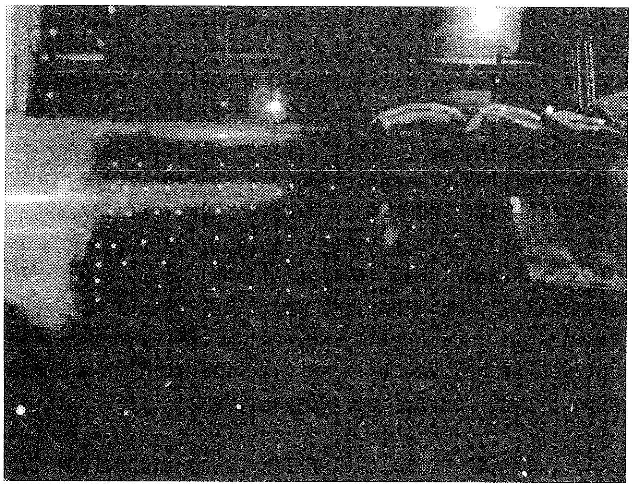

Figure 5 An image from camera 1(8.5mm lens).

to provide principal point offset, radial and tangential lens distortion parameters.

The turbine blade was statically loaded in 10 increments. At each load three sets of five convergent images were captured. Unfortunately specular reflections from the fibre glass blade surface under the bright laboratory conditions meant that target location routines developed for optimum conditions could not locate all necessary targets. An additional set of images without axial illumination were made at each load increment. Subtraction of this image from each retro-target image considerably reduced the background allowing identification of the target image points. However this method has the effect of increasing image noise, so the target locations were simply used as seed points for target measurement in the conventional retro-target images. In this way the imaged targets were automatically measured and identified on site to sub-pixel accuracy using a centre weighted algorithm (Clarke at al, 1995). Target image coordinates from the three sets of data acquired during each epoch were averaged before processing.

4. RUDIMENTARY ON-SITE VISUALISATION

Given the limited data processing power of the current image acquisition and processing system, it was not

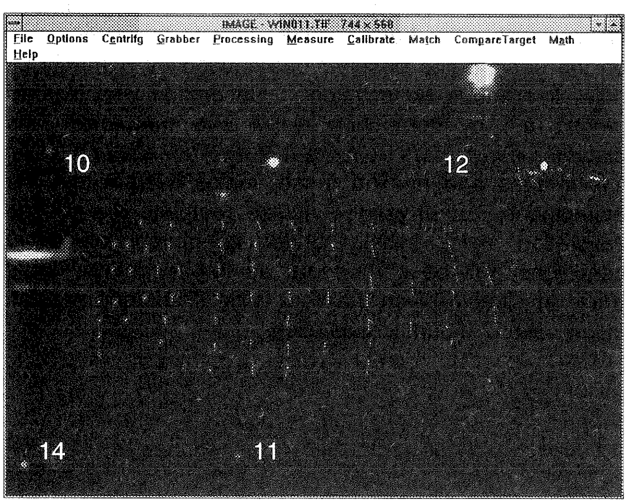

Figure 7 Image movement vectors between epochs 10 and 11 at a scale of 10x.

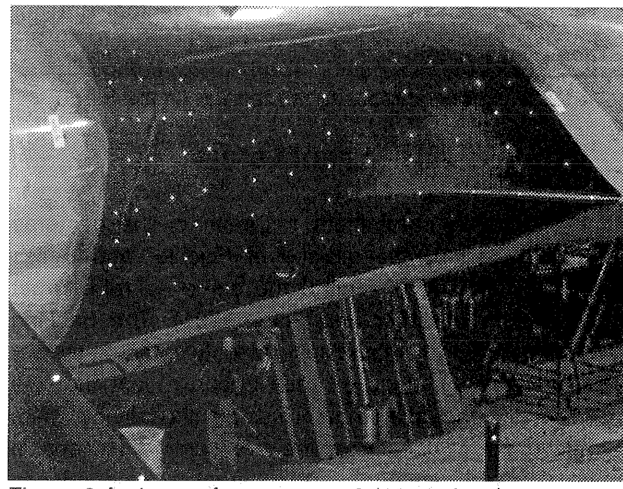

Figure 6 An image from camera 2 (16mm lens).

possible to reliably compute object space co-ordinates on-line during the experiment. Recent research work in the field of geotechnical image measurement and analysis (Chen et al 1996) has resulted in some rapid on-line target measurement and movement vector overlay procedures. By levelling the central camera it is possible to compute and draw image space movement vectors which are useful to the engineer. These can be overlaid onto the central image for on-line viewing. Figure 7 shows the image movements occurring between epochs 10 and 11. From the figure it can be seen that targets on the rotor blade have moved with respect to the camera, whilst control targets separate from the blade exhibit no movement. A display of this type can be extremely reassuring during a costly one-off experiment, it can also provide valuable information to the structural engineer. It is also possible to retrospectively analyse movements between any two image measurement sets, for any camera station. This can be very useful in checking the performance of each camera and can provide warning that a camera has been moved or knocked during the experiment so that new starting values can be computed.

Figure 8 shows similarly derived image movement vectors computed between epoch 10 and 12 where the load was increased to 175% and the angle of the jig supporting the rotor blade changed to provide sufficient ground

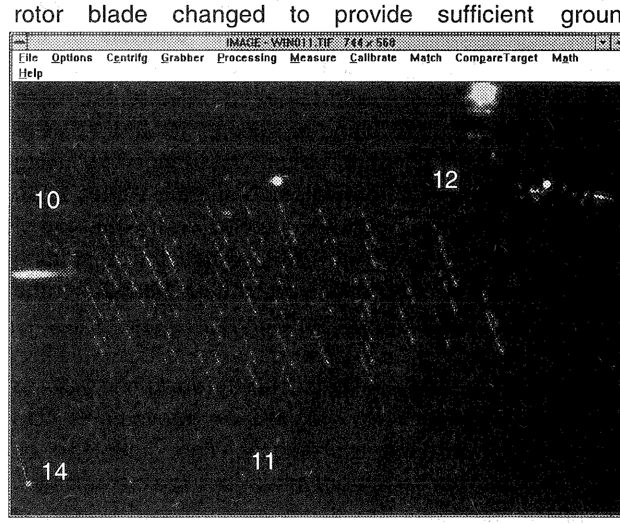

Figure 8 Image movement vectors between epochs 10 and 12 at a scale of 10x.

clearance. Obviously in this case such vectors are not useful, except to demonstrate that control points (9,10,11) appear stable and that point (14) on the supporting jig has moved in a similar direction to the targets on the blade.

5. DATA PROCESSING

Initial orientation parameters for each of the cameras were computed by the method of Fischler and Bolles using the locations of four of the surveyed retro-target control points (Fischler and Foley 1981). The tracking procedures used to automatically identify common targets between similar images at each epoch meant that the target correspondence problem was significantly reduced. Targets imaged at each of the five camera stations in epoch 10 were matched using a target correspondence algorithm developed at City University (Chen 1995). The method is founded on a three dimensional epiplanar geometry, iteratively incorporated within the bundle adjustment procedure. To avoid blunders, which can occur with dense targets and approximate camera orientation parameters, initial constraints were added to ensure that each target matched appeared on all images. As the estimates of the exterior orientation parameters were refined, the constraint was lowered to four viewpoints, and finally reduced to three viewpoints to collect any remaining unmatched targets. In this case the method correctly identified and matched all of the targets in five iterations. A common numbering scheme between all epochs could then be simply applied by cross referencing all target measurements within the appropriate images in the primary epoch. Any ambiguities caused by excessive target movement or occlusion during the course of the experiment were resolved by reapplying the epiplanar method to any remaining unlabelled target points.

During the experiment, the blade was adjusted about a pivot point so deformation could not be estimated with respect to the survey datum. Instead, deformation analysis techniques were centred on a 'free network' bundle adjustment. To commence an analysis of the movements occuring in the rotor blade, the photoco-ordinate measurements and target co-ordinate estimates of targets on the rotor blade at epochs 10 and 11 were isolated. An initial common datum was defined by using the epoch 10 target co-ordinates as starting values in an iterative least squares estimation based on the method of 'inner constraints' (Cooper, 1987). Since these starting values were final co-ordinate estimates based on the survey datum, scale was preserved.

A global congruency test (Setan 1995) (using $\alpha = 0.05$) to determine whether any significant movement had occurred between the two epochs was computed by analysis of the target co-ordinates and their associated covariance matrices. The global test indicated significant movement, so it was necessary to locate the unstable points. These were removed one at a time because the datum had to be re-defined with respect to the remaining points. A localisation procedure modified from Fraser and Gruendig (1988) was used for this purpose. The procedure consists of decomposition, re-ordering and S-transformations (Baarda 1973; Strang van Hees 1982) until the congruency test (using α=0.01) (Cooper 1987) was accepted. In this manner a group of stable points was identified. The displacements and stochastic attributes of the remaining points relative to the new datum were then derived and verified. This process was repeated as required to allow a comparison to be made between pairs of data from different epochs.

Some parameters from the adjustment computed with the 'inner constraints' epoch 10 data are shown in table 3. The RMS image co-ordinate standard deviations are derived from the mean of the measurements made from each set of three images. Since the target image quality was relatively poor, the frame averaging algorithm set a global image measurement standard deviation of 1/5th pixel.

Table 3 Some parameters from the epoch 10 adjustment

Degrees of Freedom: 333	σ_o^2: 0.220	Measurements 542	Targets 62
Axis	X	Y	Z
Target RMS (* σ_o)	0.09 mm	0.13mm	0.07 mm
Image RMS residual	0.73 μm (1/11 pixel)	0.38 μm (1/23 pixel)	---------

σ_o = standard error of an observation of unit weight.

The relatively low object space precision, 1:30,000 of the object space, is a function of network limitations imposed by the number of cameras which could be used in the system and object space restrictions on their location and orientation.

Computing a bundle adjustment including observations of straight lines at different distances gave a significantly larger variance factor, of the order of 1. This effect was isolated within the bundle adjustment to large residuals on the straight line observations caused by primarily by noisy line image observations. Calibration was instead carried out by computing radial and tangential lens distortion parameters from the mid-distance set of straight line images and holding these values fixed within the adjustment. Further work to include complete straight line calibration data, initially under controlled laboratory conditions, will be carried out as the technique could prove invaluable given the very large distortions present in low cost 'C' mount lenses used.

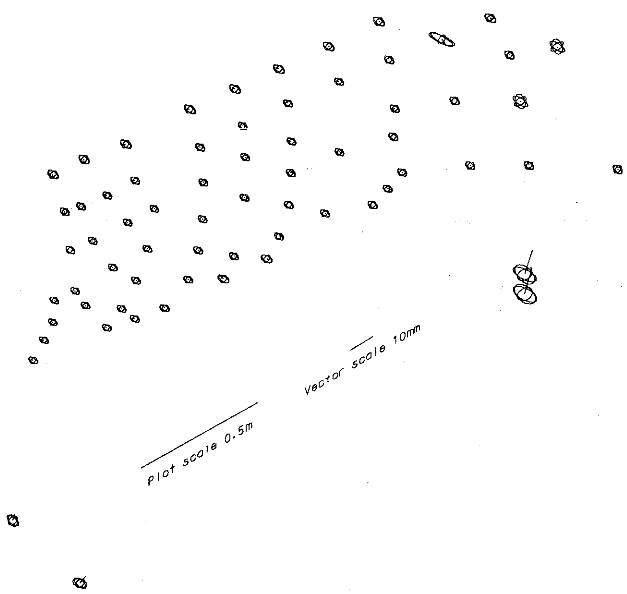

Figure 9 Isometric plot of vectors and 95% confidence ellipsoids between epochs 10 and 11

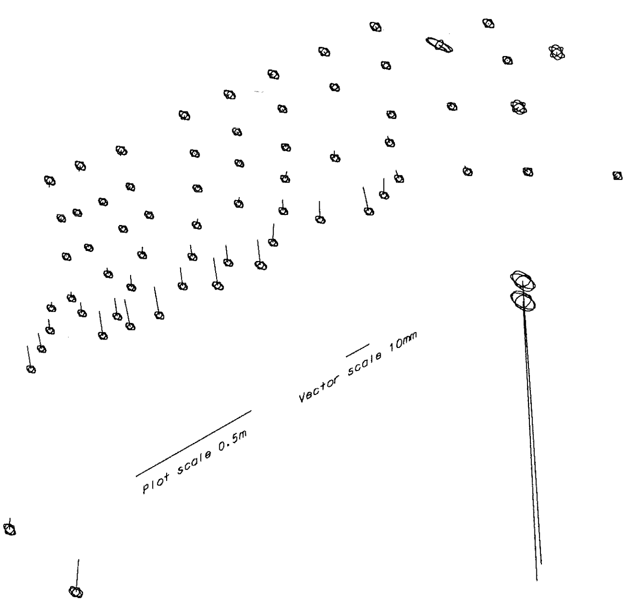

Figure 10 Isometric plot of vectors and 95% confidence ellipsoids between epochs 10 and 17.

6. ANALYSIS OF RESULTS

Computed ΔX, ΔY and ΔZ values and their associated 3D confidence regions were directly downloaded into the Integraph Microstation CAD system using in-house developed software. Figures 9 and 10 are isometric plots of 10x exaggerated target differences between: epoch 10 and 11 and; 10 and just before failure of the rotor blade during epoch 17. In figure 9, corresponding to the difference between 100% and 150% design load, no significant movement is seen on the rotor blade. The only significant movements are on the survey control points to the bottom right of the figure. Whilst these points have not physically moved, they have moved with respect to the mathematical datum defined by the congruency testing procedure. Figure 10, a comparison between epochs 10 and 17, shows significant change in shape of the rotor blade. Again the survey control points have moved with respect to the congruency datum, this time in the opposite direction since the jig angle and therefore the angle of the blade was changed many times between these two epochs. This change in angle is confirmed by movements of the target points on the jig to the bottom left of the figure. In both cases the larger ellipsoids on targets at the blade's change in section, towards the right of the view, are caused by fewer photogrammetric observations to these targets.

Figure 11, an elevation, details the movements before a failure occured outside of the targeted area towards the rotor blade tip. In this figure the upwards movements due to compression in the lower portion of this section of the rotor blade root can be clearly seen.

Finally the extraction of a profile from the data set is shown in figure 12. Here change is shown simply in exagerated vector form, but it is a simple matter to fit a new section to the data and measure for example change in section length.

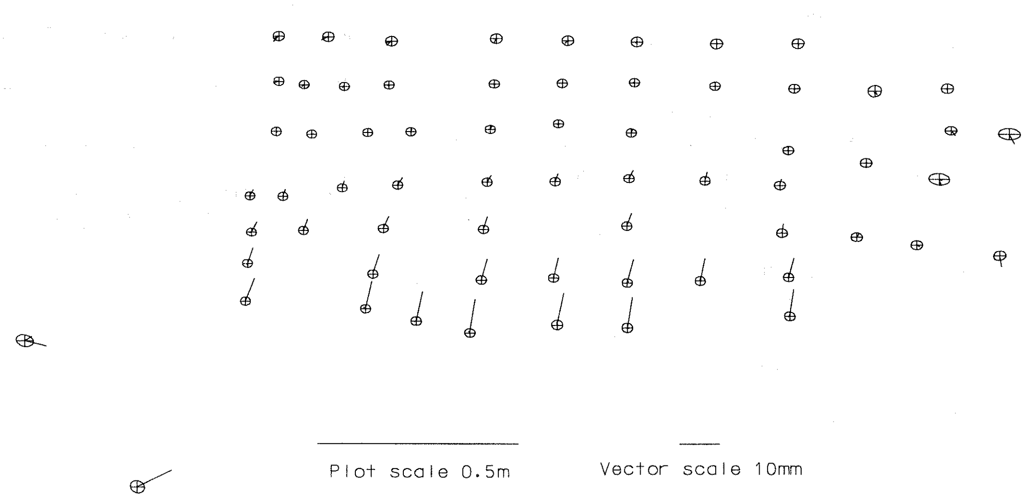

Figure 11 Elevation showing vectors and 95% confidence ellipsoids between epochs 10 and 17

Whilst such movements and measurements of change are useful to the structural engineer, the full potential of the digital photogrammetric technique can only be

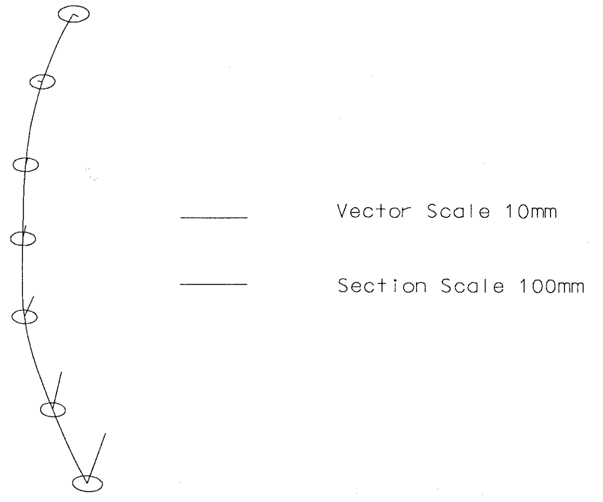

Figure 12 Exaggerated change in section of the rotor blade between epochs 10 and 17.

realised if this information is amalgamated with data from other instrumentation. A programme of structural experiments featuring research into the combination of disparate data from different instrumentation and the visualisation of pertinent engineering information thus derived is currently in progress.

7. CONCLUSIONS

In conclusion, for photogrammetry to achieve its undoubted potential in the structural testing environment, research is required to extend and adapt existing data capture, processing and visualisation technologies for on site use by engineers. Further work is necessary not only to ensure and enhance data quality, but also to provide the seamless integration of data from a wide variety of instrumentation.

This application of a low cost digital photogrammetric system to the analysis of small scale structural deformation has demonstrated the quantity of information of verifiable quality which can be rapidly obtained. There is no doubt that more can be achieved if imaging and experimental conditions are carefully designed. The rudimentary digital photogrammetric system used, whilst limited in image resolution, data acquisition rate and local computing power, has proved successful such that the key element of the project is the representation of the data in a form suitable for interpretation by the engineer. Work is currently in progress to design and build a new more powerful system which can be used to routinely monitor larger objects both in the laboratory and on site.

Work on a methodology to include the variation of lens distortion with object space which is applicable to both laboratory and uncontrolled environments is currently in progress.

8. REFERENCES

Baarda, W., 1973. S-transformations and criterion matrices. Netherlands Geodetic Commission Publications on Geodesy, New Series, 5(1). 168 pages.

Beyer,. H., 1995. Digital photogrammetry in industrial applications. International Archives of Photogrammetry and Remote Sensing. From Pixels to Sequences. 30(5W1): 373-378. March 22-24. Zurich. ISSN 0256-1840

Cooper, M.A.R., 1987. Control Surveys in Civil Engineering. Blackwells, Oxford. ISBN 0-00-383183-3. 392 pages.

Cooper, M.A.R., and Robson. S. 1994. Photogrammetric methods for monitoring deformation: Theory, practice and potential. Proceedings of the 10th Recent Advances in Experimental Mechanics, Silva Gomes et al (eds) p395-400. Balkema, Rotterdam. ISBN 90 5410 3957.

Clarke, T.A., Cooper, M.A.R., Chen, J., and Robson, S., 1995. Automatic three dimensional measurement using multiple CCD camera views. Photogrammetric Record 15(85): 27-42.

Chen, J., 1995, The use of Multiple Cameras and Geometric Constraints for 3-D Measurement, PhD Thesis, City University, UK, 245 pages.

Chen, J., Robson, S., Cooper, M.A.R., and Taylor, R.N., 1996. An Evaluation of three different image capture methods for measurement and analysis of deformation within a geotechnical centrifuge. ISPRS Congress Vienna 1996. In press.

Clarke, T.A., Robson, S., Qu, D.N., Wang, X., Cooper, M.A.R., Taylor, R.N., 1995, The Sequential Tracking of Targets in a Remote Experimental Environment, ISPRS Intercommision Workshop: From Pixels to Sequences - Sensors, Algorithms and Systems, Vol.30, 5/W1, pp.80-85.

Fischler, M.A., and Foley J.D., 1981. Random Sample Consensus: A paradigm for model fitting with applications to image analysis and automated cartography. Communications of the ACM. 24(6): pp.381- 395.

Fraser, C.S., and Gruendig, 1988. The analysis of photogrammetric deformation measurements of Turtle Mountain. Photogrammetric Engineering and Remote Sensing 51(2): pp.207-216.

Fraser, C. S. and Shortis, M. R., 1992. Variation of distortion within the photographic field. Photogrammetric Engineering and Remote Sensing, 58 (6): 851-855.

Robson, S., Brewer, A., Cooper, M.A.R., Clarke, T.A., Chen, J., Setan, H.B., and Short, T. 1995. Seeing the wood from the trees - an example of optimised digital photogrammetric deformation detection. International Archives of Photogrammetry and Remote Sensing. 30(5W1): 379-384. March 22-24. Zurich. ISSN 0256-1840.

Robson, S., and Cooper, M.A.R., 1995. Digital photogrammetric monitoring of small scale structural deformation. 3rd Symposium on Surveillance and Monitoring Surveys, University of Melbourne, Australia. pp120-130.

Setan, H., 1995. S-Transformations: A practical computational tool for deformation monitoring. 3rd Symposium on Surveillance and Monitoring Surveys, University of Melbourne, Australia. pp154-164.

Strang van Hees, G.L., 1982. Variance-covariance transformations of geodetic networks. Manuscripta Geodetica, 7(1): pp.1-20.